

## Pulsed phase modulation with harmonic electric control signal for quantum key distribution implementations

Andrei A. Gaidash<sup>1,2,a</sup>, George P. Miroshnichenko<sup>2,b</sup>, Anton V. Kozubov<sup>1,2,c</sup><sup>1</sup>SMARTS-Quanttelecom LLC, Saint Petersburg, Russia<sup>2</sup>ITMO University, Saint Petersburg, Russia<sup>a</sup>andrewdgk@gmail.com, <sup>b</sup>gpmirosh@gmail.com, <sup>c</sup>avkozubov@itmo.ru

Corresponding author: A.A. Gaidash, andrewdgk@gmail.com

**ABSTRACT** In this work, we investigate an alternative approach to phase modulation for information encoding and decoding in quantum key distribution systems. Specifically, we propose pulsed phase modulation, i.e. it has an envelope in addition to previously considered only harmonic temporal behavior of modulation index (depth), as a replacement for the conventional use of both intensity and phase modulators, which enables a more compact and cost-effective optical design. We further analyze how the principal parameters of this scheme affect the interference observed at the receiver and, consequently, their contribution to the quantum bit error rate in a subcarrier-wave quantum key distribution implementation.

**KEYWORDS** Phase modulation, quantum key distribution, subcarrier wave quantum key distribution.

**ACKNOWLEDGEMENTS** This work was done by order of JSCo Russian Railways.

**FOR CITATION** Gaidash A.A., Miroshnichenko G.P., Kozubov A.V. Pulsed phase modulation with harmonic electric control signal for quantum key distribution implementations. *Nanosystems: Phys. Chem. Math.*, 2026, **17** (1), 39–45.

### 1. Introduction

With the ongoing transition of quantum key distribution (QKD) [1] from the laboratory [2–11] to commercial deployment [12–18], research emphasis has shifted from foundational aspects toward applied implementations, including network applications [19–24]. The reliable preparation and measurement of quantum states lies at the core of any QKD protocol. In practice, the majority of QKD schemes employ weak coherent states (it can be phase-randomized [25]), where information encoding and decoding are realized using phase and intensity modulators. Commercial deployment of QKD places emphasis not only on performance but also on cost, and modulators constitute one of the most expensive elements in the transmitter (Alice) setup. It becomes even more crucial in terms of quantum networks and quantum Internet of Things. In this work, we focus on the subcarrier wave (SCW) QKD protocol [26–31], whose distinguishing feature is that information is encoded in the frequency spectrum rather than in the phase difference between spatial modes, as in conventional phase-coding schemes. In this protocol, intensity modulators are commonly used to align the prepared quantum states with the temporal gating of the detectors. Nevertheless, the phase-encoding structure of SCW QKD allows one to dispense with intensity modulation altogether. A natural solution is to replace the continuous-wave laser with a pulsed source. Yet, in practice, the implementation of such a source is nontrivial, as it requires meeting stringent conditions on both spectral width and pulse repetition rate.

To address this issue, we propose an alternative approach to phase encoding, referred to as pulsed phase modulation. We analyze the general framework of this modulation scheme and examine how its key parameters influence the resulting interference observed at the receiver and, as a consequence, contribution of their non-ideal alignments to quantum bit error rate (QBER,  $Q$ ) of a SCW QKD setup.

The article is organized as follows. In Section 2 preliminaries of phase modulation with harmonic electric control signal is considered. Section 3 is dedicated to the description of the proposed idea that modulation index can be time-dependent. In Section 4, two cases of rectangular and Gaussian shapes of modulation index envelopes are thoroughly examined. Section 5 concludes the article.

### 2. Preliminaries

Coherent state after a phase-modulation with an applied harmonic electric control signal, proportional to  $m_A \sin(\Omega t + \phi_A)$ , is as follows [27, 32]:

$$|\alpha_0\rangle_{\omega_0} \rightarrow |\psi(\phi_A)\rangle = \bigotimes_{n=-S}^S |\alpha_0 d_{0n}^S(\beta_A) e^{in\phi_A}\rangle_{\omega_n}, \quad (1)$$

where  $\alpha_0$  denotes the amplitude of initial coherent state at frequency  $\omega_0$ ,  $d_{nk}^S(\beta)$  is the Wigner d-function,  $2S + 1$  is a number of interacted frequency-modes,  $\beta_A \approx \frac{m_A}{S}$  can be considered as an efficient modulation index proportional to the amplitude of an electric control signal  $m_A$ ,  $\Omega$  and  $\phi_A$  is the frequency and the phase of the electric control signal respectively,  $\omega_n = \omega_0 + n\Omega$  is the resulting optical frequency. After the second modulation, where the electric signal is proportional to  $m_B \sin(\Omega t + \phi_B)$ , a kind of interference may be observed in the following structure of the resulting state:

$$|\psi(\phi_A, \phi_B)\rangle = \bigotimes_{n=-S}^S |\alpha_0 d_{0n}^S(\beta') e^{in\phi'}\rangle_{\omega_n}, \quad (2)$$

$$\cos(\beta') = \cos(\beta_A) \cos(\beta_B) - \sin(\beta_A) \sin(\beta_B) \cos(\phi_A - \phi_B), \quad (3)$$

and  $\phi'$  is a phase that we are not interested in.

### 3. Time-dependent modulation

Further, we explore how slow changes of modulation index, namely  $m(t_i)$ , would affect the described interference-like structure of double-modulated state. Note, we assume slowly varying envelope approximation, so that there is almost no significant change of modulation index during the time necessary for a light to travel through a modulator ( $T_{int}$ ). In other words, we divide time interval in some discrete intervals, characterized by their mean values  $t_i$ , that are comparable to the interaction time  $T_{int}$ , see Fig. 1. Thus, we treat modulation index during time interval  $t_i$  as a constant. This is necessary to assure that the model from [32] can be applied, where adiabatic process is assumed.

Other assumptions are as follows. We also consider a case of standard modulators, namely, a number of interacting modes is indefinitely large,  $S \rightarrow \infty$ . The latter implies the following approximations applied to the Eq. (3):

$$\beta(t_i) \approx \frac{m(t_i)}{S} \rightarrow 0, \quad (4)$$

$$\cos(\beta'(t_i)) \approx 1 - \frac{(\beta'(t_i))^2}{2}, \quad (5)$$

$$\cos(\beta_A(t_i)) \cos(\beta_B(t_i)) \approx 1 - \frac{\beta_A^2(t_i) + \beta_B^2(t_i)}{2}, \quad (6)$$

$$\sin(\beta_A(t_i)) \sin(\beta_B(t_i)) \approx \beta_A(t_i)\beta_B(t_i), \quad (7)$$

resulting in

$$(\beta'(t_i))^2 = \beta_A^2(t_i) + 2\beta_A(t_i)\beta_B(t_i) \cos(\phi_A - \phi_B) + \beta_B^2(t_i). \quad (8)$$

Detection of the obtained signal involves filtering out the central (initial) frequency  $\omega_0$  since the latter does not contain any phase related to the first modulation, and it only provides energy for sidebands to flow in. In turn, detection rate is proportional to the mean number of photons at sidebands  $\mu$ , that can be expressed as follows:

$$\mu = \mu_0(1 - |d_{00}^S(\beta'(t_i))|^2), \quad \mu_0 = |\alpha_0|^2. \quad (9)$$

A relation with the classical case (see Appendix A) immediately follows from the following observation and proportionality of  $\beta$  and  $m$ :

$$\lim_{S \rightarrow \infty} d_{nk}^S(\beta) = J_{n-k}(m), \quad (10)$$

where  $J_n(m)$  is the Bessel function of the first kind. Thus,

$$\mu = \mu_0(1 - J_0^2(m'(t_i))), \quad (11)$$

$$m'(t_i) = \sqrt{m_A^2(t_i) + 2m_A(t_i)m_B(t_i) \cos(\phi_A - \phi_B) + m_B^2(t_i)}. \quad (12)$$

Also, if  $\max_{t_i}(m(t_i)) \ll 1$ , that is a common value for an SCW QKD system, then the following approximation of Bessel function takes place:

$$\mu \approx \mu_0 \frac{(m'(t_i))^2}{2}. \quad (13)$$

In addition, further we consider energetic characteristics of an optical signal depending on a phase difference  $\phi_A - \phi_B$  proportional to the following form:

$$E(\phi_A - \phi_B) \sim \sum_{i=-\infty}^{\infty} (m'(t_i))^2. \quad (14)$$

For the sake of simplicity, it is more convenient to consider dependencies on continuous time (assuming interaction time  $T_{int}$  rather small). Hereinafter, we assume the following substitution, see Fig. 1:

$$E(\phi_A - \phi_B) \sim \sum_{i=-\infty}^{\infty} (m'(t_i))^2 \rightarrow \int_{-\infty}^{\infty} (m'(t))^2 dt. \quad (15)$$

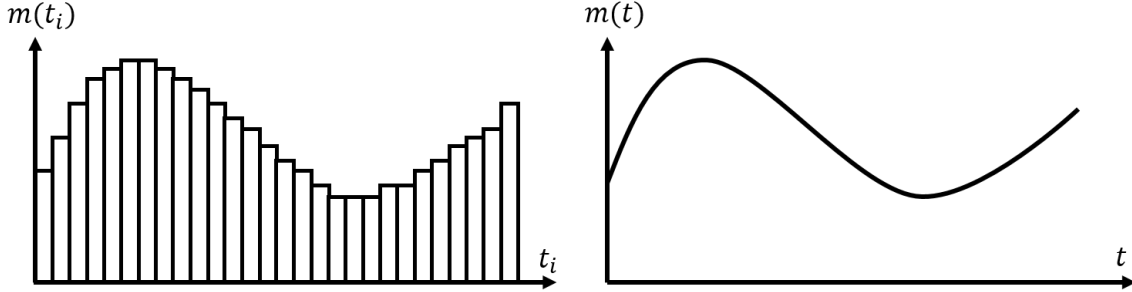


FIG. 1. **Left:** visualization of slow change of modulation index  $m(t_i)$  with respect to chosen time-intervals  $t_i$ ,  $t_{i+1} - t_i \approx T_{int}$ , where the latter is the time necessary for a light to travel through a modulator; we assume small amount of change of modulation index during  $T_{int}$ . **Right:** for the sake of simplicity, it is more convenient to consider dependence of modulation index  $m(t)$  on continuous time, assuming interaction time  $T_{int}$  rather small, and allowing approximation as in Eq. (15)

#### 4. Special cases

Further, in the section, several special cases of specific time-dependent  $m(t)$  will be considered. In particular, pulse-shaped modulation is relevant in SCW QKD. It can be viewed as an alternative to pulse generation provided by an amplitude modulator, so the latter is no longer necessary. At this point, influence of relative shape difference for modulation-pulses on QBER, namely

$$Q = \frac{E(\pi)}{E(0) + E(\pi)}, \quad (16)$$

where  $E(\phi_A - \phi_B)$  is the total energy of detected optical signal dependent on the phase difference between two modulation signals, should be investigated. Without loss of generality, shapes of pulses can be estimated without absolute values but with relative scaling as well as  $E(\phi_A - \phi_B)$  can be estimated up to a common factor due to  $Q$  is a ratio.

##### 4.1. Rectangular pulses

Consider rectangular modulation pulse:

$$m_A(t) = \text{rect}(t) = \Theta\left(t + \frac{1}{2}\right) - \Theta\left(t - \frac{1}{2}\right), \quad (17)$$

$$m_B(t) = x \text{rect}\left(\frac{t - \Delta t}{y}\right) = x\left(\Theta\left(t - \Delta t + \frac{y}{2}\right) - \Theta\left(t - \Delta t - \frac{y}{2}\right)\right), \quad (18)$$

where  $\Theta(t)$  is the Heaviside function,  $0 \leq x \leq 1$  denotes mismatch of modulation amplitude,  $y \geq 0$  denotes pulse-width mismatch, and  $\Delta t \geq 0$  is time-shift. Considering Eq. (13) as the mean photon number per time, total amount of energy at sidebands in pulse is proportional to the following integral, where Eq. (12) is used:

$$E(\phi_A - \phi_B) \sim \int_{-\infty}^{\infty} (m'(t))^2 dt = 1 + x^2 y + 2x f(\Delta t, y) \cos(\phi_A - \phi_B), \quad (19)$$

where

$$f(\Delta t, y) = \begin{cases} 0, & \Delta t \geq \frac{y+1}{2} \\ y, & \Delta t \leq \frac{|y-1|}{2} \text{ and } y \leq 1 \\ 1, & \Delta t \leq \frac{|y-1|}{2} \text{ and } y \geq 1 \\ \frac{1}{2} + \frac{y}{2} - \Delta t, & \frac{|y-1|}{2} \leq \Delta t \leq \frac{y+1}{2} \end{cases}. \quad (20)$$

Finally, QBER can be estimated as follows:

$$Q = \frac{1}{2} - \frac{x f(\Delta t, y)}{1 + x^2 y}. \quad (21)$$

Further, we will consider several special cases in order to determine influence of each parameter mismatch on  $Q$ .

- (1) Mismatch of only modulation amplitude of the envelope implies that  $y = 1$  and  $\Delta t = 0$ . Then,

$$Q(x) = \frac{(1-x)^2}{2(1+x^2)}, \quad (22)$$

which is well agreed with the known case, where  $m_A \neq m_B$  and both are constants. The latter dependence is shown in Fig. 2(a). Observe, that

$$Q\left(\frac{1}{x}\right) = Q(x). \quad (23)$$

Also, for a small modulation depth mismatch, i.e.  $|x-1| \ll 1$ , the following approximation takes place:

$$Q(x) \approx \frac{(1-x)^2}{4}; \quad (24)$$

- (2) Mismatch of only pulse-width,  $x = 1$  and  $\Delta t = 0$ , yields as follows:

$$Q(y) = \left| \frac{y-1}{2(1+y)} \right| = Q\left(\frac{1}{y}\right), \quad (25)$$

and it is shown in Fig. 2(b);

- (3) Displacement in time with  $x = 1$  and  $y = 1$  results in the following expression:

$$Q(\Delta t) = \begin{cases} \frac{\Delta t}{2}, & \Delta t \leq 1 \\ \frac{1}{2}, & \Delta t \geq 1 \end{cases}. \quad (26)$$

The obtained dependence is shown in Fig. 2(c).

#### 4.2. Gaussian pulses

Consider Gaussian-shaped modulation pulse:

$$m_A(t) = \frac{1}{\sqrt{2\pi}} e^{-\frac{t^2}{2}}, \quad (27)$$

$$m_B(t) = \frac{x}{\sqrt{2\pi y}} e^{-\frac{(t-\Delta t)^2}{2y^2}}, \quad (28)$$

where  $x \geq 0$  denotes mismatch of modulation amplitude,  $y \geq 0$  denotes pulse-width mismatch, and  $\Delta t$  is time-shift. In this case, the total amount of energy in the pulse is as follows:

$$E(\phi_A - \phi_B) \sim \int_{-\infty}^{\infty} (m'(t))^2 dt \sim 1 + \frac{x^2}{y} + \frac{x\sqrt{2}e^{-\frac{(\Delta t)^2}{2(1+y^2)}}}{\sqrt{y^2+1}} \cos(\phi_A - \phi_B), \quad (29)$$

where we are not interested in common factors to be neglected. Thus,

$$Q = \frac{1}{2} - \frac{xy\sqrt{2}e^{-\frac{(\Delta t)^2}{2(1+y^2)}}}{(y+x^2)\sqrt{y^2+1}}. \quad (30)$$

Dependencies of  $Q$  on each misalignment are as follows:

- (1) Mismatch of modulation depth  $x$  with  $y = 1$  and  $\Delta t = 0$  dictates the same dependence as in the previous case of rectangular pulse, that is shown in Fig. 2(a);  
 (2) Pulse-width mismatch (with  $x = 1$  and  $\Delta t = 0$ ) results in the following dependence:

$$Q(y) = \frac{1}{2} - \frac{y\sqrt{2}}{(y+1)\sqrt{y^2+1}} = Q\left(\frac{1}{y}\right). \quad (31)$$

It is shown in Fig. 2(d) and can be approximated as follows in case of small deviations, i.e.  $|y-1| \ll 1$ ,

$$Q(y) \approx \frac{3}{16}(y-1)^2; \quad (32)$$

- (3) Time-shift of one Gaussian relative to another, assuming  $y = 1$  and  $x = 1$ , contributes to  $Q$  as follows:

$$Q(\Delta t) = \frac{1 - e^{-\frac{(\Delta t)^2}{4}}}{2}. \quad (33)$$

The latter is shown in Fig. 2(e); in case of small time-shift  $|\Delta t| \ll 1$ , it has the following approximation:

$$Q(\Delta t) \approx \frac{(\Delta t)^2}{8}. \quad (34)$$

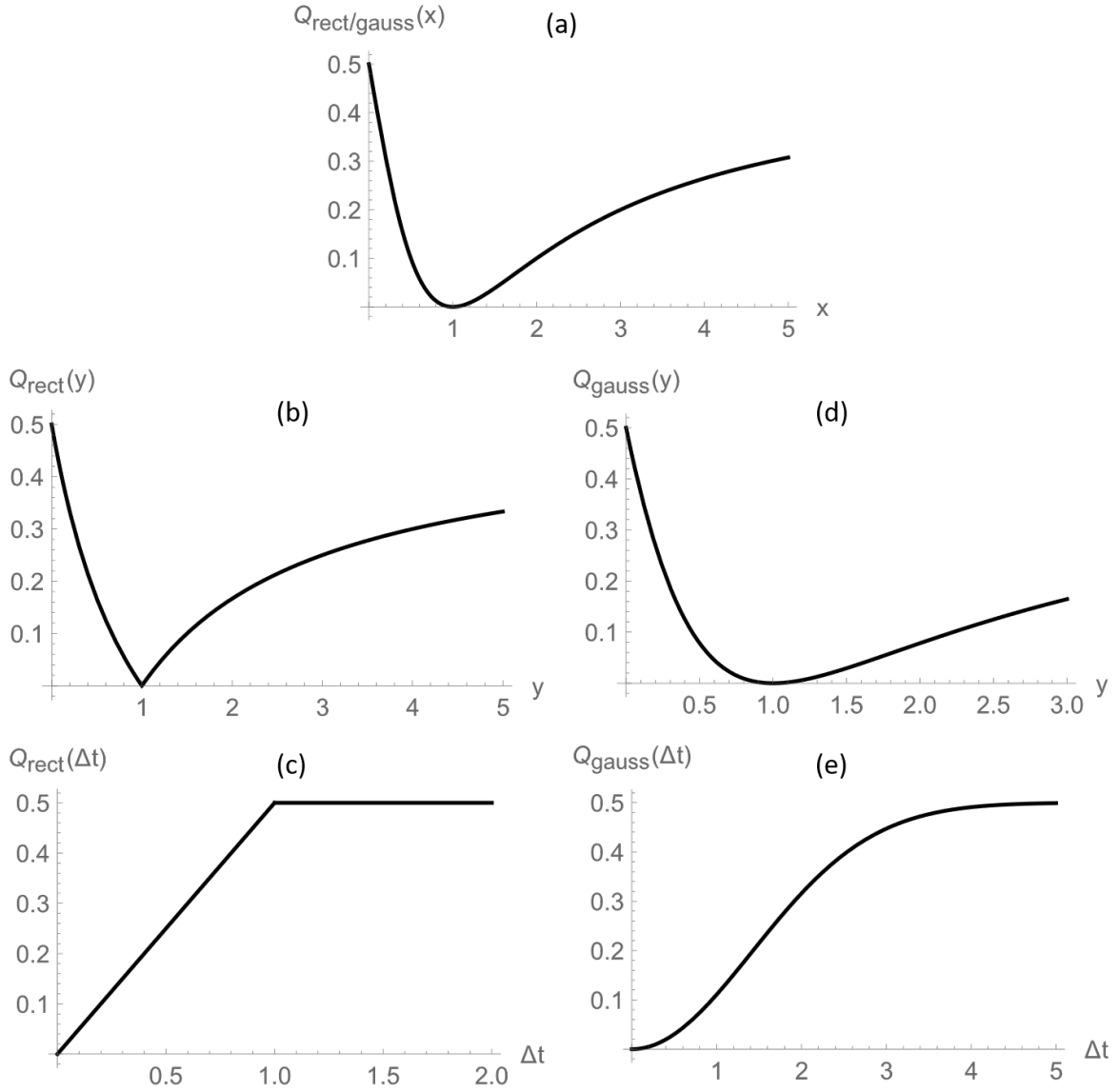


FIG. 2. Graphical representation of estimated QBER value  $Q$  dependent on various parameters of modulation-pulse shape: (a) according to Eq. (22) for both Gaussian and rectangular pulse shapes, (b) according to Eq. (25) for rectangular pulse shape, (c) according to Eq. (26) for rectangular pulse shape, (d) according to Eq. (31) for Gaussian pulse shape, (e) according to Eq. (33) for Gaussian pulse shape

## 5. Discussion and conclusion

In the article, utilization of time-dependent (pulsed) modulation index in a phase modulation with harmonic electric control signal is proposed, especially for implementation in SCW QKD systems. Due to the latter, necessity of an additional intensity modulation is absent. It is required that both sender's and receiver's pulses should be equal, that is not always true for a practical implementation. In the paper, we have examined how misalignment of these pulses (modulation depth scaling  $x$ , relative width  $y$ , and relative time-shift  $\Delta t$ ) affect the QBER value, one of the most crucial characteristics for a QKD device. Obtained dependencies may be used in order to retrospectively estimate admissible bounds for misalignment parameters in case of a given QBER threshold.

Two types of pulse shapes were considered: rectangular and Gaussian, as the most simple examples. Despite the real pulse may have slightly more peculiar envelope, obtained dependencies, shown in Fig. 2, for a given examples share general features. Nonetheless, results, provided in Eqs. (11) and (12), are of a general form suited for any temporal envelope shapes of modulation index. However, during the derivation of the resulting expressions we employ several assumptions in regard of adiabatic dynamical regime, that should be met. In particular, a too rapid change of modulation index may break the mentioned assumptions and, as a result, this scenario should be considered properly. We believe, that described rapid changes may result in temporal delay between controlling electrical signal and actual change of refraction

index that causes modulation. Namely, change of refraction index do not catch up with applied electric field. Rigorous study of this problem requires thorough examination of the quasi-energy operator's eigenvalues behavior that is far beyond of the article's scope, leaning towards practical implementation.

In addition, the obtained results can be viewed as a transition of optical transformations, e.g. action of intensity modulator, to the domain of electrical ones, e.g. manipulation of modulation index envelope. From the perspective, various families of these manipulations with applied to the crystal electric field can be considered further. In particular, what kind of modulation is required in order to simulate the action of an optical filter? Or is it possible to concentrate energy in spectrum closer to the central frequency? The problem of several harmonics multiplexing is also of interest. Provided expressions (11) and (12) are the first step forward in solving these problems that may result in significant simplifications of QKD optical schemes and vastly improving their performance in various ways.

### A. Appendix: Classical phase modulation with harmonic electric control signal

Classical approach for phase modulation with harmonic electric control signal is rather straightforward and well known. Consider the optical signal as a plane-wave, i.e.  $Ae^{i\omega t}$ , that traverses a crystal with changing refraction index due to applied external electric field. Namely, plane-wave obtains phase-shift (proportional to)  $m \sin(\Omega t + \phi_1)$ . Using the Jacobi-Anger expansion formula,

$$e^{iz \cos(\theta)} = \sum_{n=-\infty}^{\infty} J_n(m) e^{in\theta}, \quad (35)$$

the expression for the modulated light is as follows:

$$Ae^{i\omega t} e^{im \sin(\Omega t + \phi_1)} = \sum_{n=-\infty}^{\infty} (AJ_n(m) e^{in\phi_1}) e^{i(\omega + n\Omega)t}, \quad (36)$$

where  $AJ_n(m)$  and  $n\phi_1$  can be considered as amplitude and phase, respectively, of a plane-wave with frequency  $\omega + n\Omega$ . If one utilizes a second modulator with modulation index  $m \sin(\Omega t + \phi_2)$ , that differs only in phase, then the total energy (or power) of all sidebands ( $n \neq 0$ ) is proportional to

$$\begin{aligned} & \sum_{n \neq 0} |(AJ_n(m_0) e^{in\phi_0}) e^{i(\omega + n\Omega)t}|^2 = \\ & = |A|^2 (1 - J_0^2(2m \cos(\frac{\phi_1 - \phi_2}{2}))) = \\ & |A|^2 (1 - J_0^2(m \sqrt{2(1 + \cos(\phi_1 - \phi_2))})), \end{aligned} \quad (37)$$

where we have used identities given by

$$\begin{aligned} & |Ae^{i\omega t} e^{im \sin(\Omega t + \phi_1)} e^{im \sin(\Omega t + \phi_2)}|^2 = \\ & = |Ae^{i\omega t} e^{i(2m \cos(\frac{\phi_1 - \phi_2}{2}) \sin(\Omega t + \frac{\phi_1 + \phi_2}{2}))}|^2 = \\ & \left[ m_0 \equiv 2m \cos(\frac{\phi_1 - \phi_2}{2}), \quad \phi_0 \equiv \frac{\phi_1 + \phi_2}{2} \right] \\ & = |Ae^{i\omega t} e^{i(m_0 \sin(\Omega t + \phi_0))}|^2. \end{aligned} \quad (38)$$

Expression (37) is fully agreed with Eq. (11) and (12) in this simple example, where modulation index  $m$  is constant.

### References

- [1] Pirandola S., Andersen U.L., Banchi et al. Advances in quantum cryptography. *Advances in optics and photonics*, 2020, **12**(4), P. 1012–1236.
- [2] Bennett C.H., Bessette F., Brassard G., Salvail L., Smolin J. Experimental quantum cryptography. *Journal of cryptology*, 1992, **5**(1), P. 3–28.
- [3] Townsend P.D. Experimental investigation of the performance limits for first telecommunications-window quantum cryptography systems. *IEEE Photonics Technology Letters*, 2002, **10**(7), P. 1048–1050.
- [4] Gui Y.Z., Han Z.F., Mo X.F., Guo G.C. Experimental quantum key distribution over 14.8 km in a special optical fibre. *Chin. Phys. Lett.*, 2003, **20**(5), P. 608–610.
- [5] Marand C., Townsend P. D. Quantum key distribution over distances as long as 30 km. *Optics Letters*, 1995, **20**(16), P. 1695–1697.
- [6] Hughes R.J., Morgan G.L., Peterson C.G. Quantum key distribution over a 48 km optical fibre network. *Journal of Modern Optics*, 2000, **47**(2-3), P. 533–547.
- [7] Weier H. Experimental quantum cryptography. *Diploma Dissertation, Technical University of Munich*, 2003.
- [8] Tittel W., Zbinden H., Gisin N. Experimental demonstration of quantum secret sharing. *Physical Review A*, 2001, **63**(4), P. 042301.
- [9] Stucki D., Gisin N., Guinnard O., Ribordy G., Zbinden H. Quantum key distribution over 67 km with a plug&playsystem. *New Journal of Physics*, 2002, **4**(1), P. 41.
- [10] Buttler W.T., Hughes R.J., Lamoreaux S.K., Morgan G.L., Nordholt J.E., Peterson C.G. Daylight quantum key distribution over 1.6 km. *Physical Review Letters*, 2000, **84**(24), P. 5652.
- [11] Buttler W.T., Hughes R.J., Kwiat P.G., Lamoreaux S.K., Luther G.G., Morgan G.L., et al. Practical free-space quantum key distribution over 1 km. *Physical Review Letters*, 1998, **81**(15), P. 3283.

- [12] Pljonkin A., Singh P.K. The review of the commercial quantum key distribution system. *Fifth International Conference on Parallel, Distributed and Grid Computing (PDGC) by IEEE*, 2018, P. 795–799.
- [13] Oesterling L., Hayford D., Friend G. Comparison of commercial and next generation quantum key distribution: Technologies for secure communication of information. *Conference on Technologies for Homeland Security (HST) by IEEE*, 2012, P. 156–161.
- [14] Makarov V., Abrikosov A., Chaiwongkhot P., Fedorov A.K., Huang A., Kiktenko E., et al. Preparing a commercial quantum key distribution system for certification against implementation loopholes. *Physical Review Applied*, 2024, **22**(4), P. 044076.
- [15] Al Natsheh A., Gbadegeshin S.A., Rimpiläinen A., Imamovic-Tokalic I., Zambrano, A. Identifying the challenges in commercializing high technology: A case study of quantum key distribution technology. *Technology Innovation Management Review*, 2015, **5**(1).
- [16] Cavaliere F., Prati E., Poti L., Muhammad I., Catuogno T. Secure quantum communication technologies and systems: From labs to markets. *Quantum Reports*, 2020, **2**(1), P. 80–106.
- [17] Sasaki M., Fujiwara M., Ishizuka H., Klaus W., Wakui K., Takeoka M., et al. Field test of quantum key distribution in the Tokyo QKD Network. *Optics express*, 2011, **19**(11), P. 10387–10409.
- [18] Chaiwongkhot P., Sajeed S., Lydersen L., Makarov, V. Finite-key-size effect in a commercial plug-and-play QKD system. *Quantum Science and Technology*, 2017, **2**(4), P. 044003.
- [19] Cao Y., Zhao Y., Wang Q., Zhang J., Ng S.X., Hanzo L. The evolution of quantum key distribution networks: On the road to the qinternet. *IEEE Communications Surveys & Tutorials*, 2022, **24**(2), P. 839–894.
- [20] Mehic M., Niemiec M., Rass S., Ma J., Peev M., Aguado A., et al. Quantum key distribution: a networking perspective. *ACM Computing Surveys (CSUR)*, 2020, **53**(5), P. 1–41.
- [21] Sharma P., Agrawal A., Bhatia V., Prakash S., Mishra A.K. Quantum key distribution secured optical networks: A survey. *IEEE Open Journal of the Communications Society*, 2021, **2**, P. 2049–2083.
- [22] Peev M., Pacher C., Alléaume R., Barreiro, C., Bouda J., Boxleitner W., et al. The SECOQC quantum key distribution network in Vienna. *New journal of physics*, 2009, **11**(7), P. 075001.
- [23] Dianati M., Alléaume R., Gagnaire M., Shen X. Architecture and protocols of the future European quantum key distribution network. *Security and Communication Networks*, 2008, **1**(1), P. 57–74.
- [24] Dervisevic E., Tankovic A., Fazel E., Kompella R., Fazio P., Voznak M., Mehic M. Quantum Key Distribution Networks-Key Management: A Survey. *ACM Computing Surveys*, 2025, **57**(10), P. 1–36.
- [25] Guselnikov M.S., Gaidash A.A., Miroshnichenko G.P., Kozubov A.V. Properties of multi-moded phase-randomized coherent states. *Nanosystems: Physics, Chemistry, Mathematics*, 2025, **16**(3), P. 311–316.
- [26] Gaidash A., Miroshnichenko G., and Kozubov A. Subcarrier wave quantum key distribution with leaky and flawed devices. *Journal of the Optical Society of America B*, 2022, **39**(2), P. 577–585.
- [27] Miroshnichenko G., Kozubov A., Gaidash A., Gleim A.V., and Horoshko D.V. Security of subcarrier wave quantum key distribution against the collective beam-splitting attack. *Optics express*, 2018, **26**(9), P. 11292–11308.
- [28] Sajeed Sh., Chaiwongkhot P., Huang A., Qin H., Egorov V., Kozubov A., Gaidash A., Chistiakov V., Vasiliev V., Gleim A., et al. An approach for security evaluation and certification of a complete quantum communication system. *Scientific Reports*, 2021, **11**(1), P. 1–16.
- [29] Chistiakov V., Kozubov A., Gaidash A., Gleim A., and Miroshnichenko G. Feasibility of twin-field quantum key distribution based on multi-mode coherent phase-coded states. *Optics express*, 2019, **27** (25), P. 36551–36561.
- [30] Samsonov E., Goncharov R., Gaidash A., Kozubov A., Egorov V., and Gleim A. Subcarrier wave continuous variable quantum key distribution with discrete modulation: mathematical model and finite-key analysis. *Scientific Reports*, 2020, **10** (1), P. 1–9.
- [31] Latypov I.Z., Chistyakov V.V., Fadeev M.A., Sulimov D.V., Khalturinsky A.K., Kynev S.M., Egorov V.I. Hybrid quantum communication protocol for fiber and atmosphere channel. *Nanosystems: Physics, Chemistry, Mathematics*, 2024, **15**(5), P. 654–657.
- [32] Miroshnichenko G., Kiselev A., Trifanov A., Gleim A. Algebraic approach to electro-optic modulation of light: exactly solvable multimode quantum model. *Journal of the optical society of America B*, 2017, **34**(6), P. 1177–1190.

---

Submitted 9 November 2025; revised 9 December 2025; accepted 11 December 2025

#### Information about the authors:

Andrei A. Gaidash – SMARTS-Quanttelecom LLC, 199178, 59-1-B 6th line of Vasilievsky island, Saint Petersburg, Russia; ITMO University, 3b Kadetskaya Line, 199034 Saint Petersburg, Russia; ORCID 0000-0001-9870-9285; andrewdgk@gmail.com

George P. Miroshnichenko – ITMO University, 3b Kadetskaya Line, 199034 Saint Petersburg, Russia; ORCID 0000-0002-4265-8818; gpmirosh@gmail.com

Anton V. Kozubov – SMARTS-Quanttelecom LLC, 199178, 59-1-B 6th line of Vasilievsky island, Saint Petersburg, Russia; ITMO University, 3b Kadetskaya Line, 199034 Saint Petersburg, Russia; ORCID 0000-0002-4468-5406; avkozubov@itmo.ru

Conflict of interest: the authors declare no conflict of interest.